Development of the Mars microbeam Raman spectrometer (MMRS)

Alian Wang,[1] Larry A. Haskin,[1] Arthur L. Lane,[2] Thomas J. Wdowiak,[4]
Steven W. Squyres,[5] Robert J. Wilson,[3] Larry E. Hovland,[3] Ken S. Manatt,[2]
Nasrat Raouf,[3] and Christopher D. Smith[6]

Received 6 March 2002; revised 18 June 2002; accepted 3 July 2002; published 30 January 2003.

[1] Raman spectroscopy is a powerful tool for mineral characterization and for detection of water and organic and inorganic forms of carbon. The Mars microbeam Raman spectrometer (MMRS) is designed for close-up analysis of rocks and soils in planetary surface exploration. The MMRS consists of a probe (in a flight unit to be deployed by a robotic arm) and a spectrograph, laser source, and electronics (in a flight unit to reside on a rover or lander). The Raman probe has a scanning optical bench that enables a 1-cm linear traverse across a target rock or soil, both on target materials as encountered and on fresh surfaces of rocks exposed by abrasion or coring. From these spectra, one can identify major, minor, and trace minerals, obtain their approximate relative proportions, and determine chemical features (e.g., Mg/Fe ratio) and rock textural features (e.g., mineral clusters, amygdular fill, and veins). One can also detect and identify organic species, graphitic carbon, and water-bearing phases. Extensive performance tests have been done on a brassboard model of the MMRS using a variety of geological materials (minerals, rocks, Martian meteorites, etc.). These tests show that a Raman spectrometer can be built that is suitably miniaturized, sufficiently robust, and low enough in power usage to serve as an on-surface planetary instrument, yet the spectrometer can retain high detection sensitivity and yield near laboratory quality spectra over a broad wavelength range. These features are essential to provide definitive mineralogy in a planetary exploration. *INDEX TERMS:* 3672 Mineralogy and Petrology: Planetary mineralogy and petrology (5410); 3694 Mineralogy and Petrology: Instruments and techniques; 3994 Mineral Physics: Instruments and techniques; 5494 Planetology: Solid Surface Planets: Instruments and techniques; *KEYWORDS:* Raman spectroscopy, Mars in-situ mineralogy, Planetary on-surface mineral identification, Water on Mars, Miniaturized Raman spectrometer, Mars Microbeam Raman Spectrometer

Citation: Wang, A., L. A. Haskin, A. L. Lane, T. J. Wdowiak, S. W. Squyres, R. J. Wilson, L. E. Hovland, K. S. Manatt, N. Raouf, and C. D. Smith, Development of the Mars microbeam Raman spectrometer (MMRS), *J. Geophys. Res.*, *108*(E1), 5005, doi:10.1029/2002JE001902, 2003.

1. Introduction

[2] Exploration of Mars for the near future will emphasize themes of "life, water, and environment" [*EPO-NASA*, 1995]. Successful pursuit of these themes can benefit from definitive, detailed knowledge of the mineralogy of Martian surface materials and a search for water and organic carbon. "Definitive" mineralogy means unambiguous identification of minerals, determination of proportions of different minerals in rocks or soils, and determination of chemical compositions of minerals. From detailed mineralogy, we can discover past Martian environmental conditions. Such conditions may include subaerial alteration of rock surfaces, fluvial and marine alteration and deposition, and hydrothermal alteration and deposition, as well as the planet's early igneous chemical differentiation. By combining information about past environments with information about Martian organic carbon and inorganic reduced carbon, we can speculate rationally on the possible development of life on Mars and better assess the possibility of retention of fossils, particularly microbial ones.

[3] The most definitive studies of mineralogy of Martian materials, including evidence regarding the issue of life, will take place in laboratories on Earth, once sample-return missions take place. Meanwhile, in situ analysis of mineralogy using visible, IR, and Mössbauer spectroscopy is planned for upcoming missions (instruments similar to those described by *Squyres et al.* [1999], *Christensen et al.* [2001], and *Rieder et al.* [1997]). In this paper, we

[1]Department of Earth and Planetary Sciences and McDonnell Center for the Space Sciences, Washington University, St. Louis, Missouri, USA.
[2]Earth and Space Sciences Division, Jet Propulsion Laboratory, Pasadena, California, USA.
[3]Observational Systems Division, Jet Propulsion Laboratory, Pasadena, California, USA.
[4]Department of Physics, University of Alabama at Birmingham, Birmingham, Alabama, USA.
[5]Center for Radiophysics and Space Physics, Cornell University, Ithaca, New York, USA.
[6]Engineering Services, Swales Aerospace Corp., Pasadena, California, USA.

Copyright 2003 by the American Geophysical Union.
0148-0227/03/2002JE001902$09.00

present an alternative method for on-surface determination of mineralogy and to assist in sample selection: microbeam Raman spectroscopy [*Wang et al.*, 1995]. This method is rapid and sensitive. It provides information about chemical bonding and crystal structure, and thus enables direct identification of oxyanionic minerals (SiO_4^{4-}, CO_3^{2-}, SO_4^{2-}, PO_4^{3-}, etc.), oxide and sulfide minerals (FeOOH, Fe_2O_3, Fe_3O_4, FeS, FeS_2, TiO_2, etc.), water and water-bearing minerals (ice, $CaSO_4 \cdot 2H_2O$, micas, clay minerals, clathrates, etc.) and organic and inorganic carbon [*Wang et al.*, 1994]. It can provide information on rock texture, and it can determine cation ratios in many minerals.

[4] Our implementation of Raman spectroscopy includes scanning across the target surface with a microbeam, which enables statistical estimates of relative abundance for major minerals and detection of minor and trace minerals. The purpose of this paper is to present the performance of a Raman microanalytical instrument, the Mars microbeam Raman spectrometer (MMRS), which has been designed as a prototype instrument for a landed Mars mission. The prototype instrument shows that a space flight version of the instrument can be simple, robust, low mass, small volume, conservative of power, and able to work in the harsh environments encountered by flight instruments. The prototype instrument has the sensitivity and spectral range and quality that approach those of a modern laboratory Raman instrument. It can scan unmodified surfaces of rocks and soils as encountered, without sample preparation, as well as examine abraded rock surfaces and cores. Here, we report the characteristics and testing of the current model (''brassboard'') of this miniaturized Raman system to indicate the potential of this technique. The brassboard is based on a less sophisticated ''breadboard'' instrument described previously [*Wang et al.*, 1998a].

2. Characteristics and Development of the MMRS

[5] The MMRS has a probe, in the space flight version to be deployed by the robotic arm of a rover or lander; and a spectrograph, a laser, and electronics (including a microprocessor) to be mounted on or in the body of the rover or lander. Electrical cables will extend from the rover to the probe for power and monitoring, and optical fibers will connect the probe and the spectrograph for signal transfer.

[6] The MMRS brassboard, described here, tests these configurations. The brassboard probe dimensions are $\sim$5.7 $\times$ 7.0 $\times$ 7.5 cm (Figure 1a), and the brassboard spectrograph dimensions are $\sim$11.5 $\times$ 14.0 $\times$ 5.9 cm (Figure 1b); the flight MMRS probe and spectrograph are expected to be the same size or slightly smaller. A schematic diagram of the system is shown in Figure 2. For the MMRS brassboard described here, it was premature to produce the electronic boards in miniaturized form, because the nature of the rover or lander accommodations are not yet known, but they can fit within dimensions of 20 $\times$ 15 $\times$ 8 cm, based on our preliminary engineering design. The laser and its power supply have also not been miniaturized, but will have dimensions $\sim$3 $\times$ 3 $\times$ 5 cm, based on dimensions of commercial devices. The total mass of the MMRS system is $\sim$2.5 kg, of which the mass of the probe is just under 200 g. Operationally, the MMRS probe will be positioned against the target at a time convenient to the deploying host system, and it will collect spectra during the Mars early night. A set of 50–200 Raman spectra will be taken from the target during a 1–4-hour period. Total energy usage is estimated to be $\sim$35 Wh for a set of 100 spectra.

[7] Our Raman system was designed to satisfy two extremes. On the one hand, like any flight instrument, it needs to be simple, robust, low mass, economical of power, and able to work in a harsh environment. It must be stable against the mechanical stresses of launch, landing, rover travel, and arm deployment. The probe must function properly under harsh environmental conditions that include daily temperature cycling over a range of $\sim$100°C, nighttime operation at low temperature (as low as $-$60°C), low atmospheric pressure, and irradiation by cosmic rays. On the other hand, to achieve the goals of mineral characterization, an on-surface Raman system should cover a broad spectral region and have adequate spectral resolution and detection sensitivity. Our system covers the range 200–1800 cm^{-1} for characterization of minerals and graphitic carbon, and 2500–4000 cm^{-1} for detection of organic functional groups and water. Our instrument design called for a spectral resolution of $\sim$7 cm^{-1} to give a wave number precision of $\leq$2 cm^{-1} for peak positions; this was nearly achieved, and that resolution is shown to be adequate for our measurements. The probe delivers $\sim$10 mW of laser power to the target. To achieve a high tolerance of the relief intrinsic to unprepared, rough sample surfaces (rock or soils) without an autofocus mechanism, the probe has a large depth-of-sampling field. To obtain a line of 100 spectra along a 1.2-cm traverse of the target surface, the probe uses a simple line-scan mechanism. Combining a microbeam with a line-scanning traverse capability increases the probability of finding minor minerals and weak Raman scattering phases because the spectrum obtained at most spots will be of only one or two minerals. The overall result of such a line scan is thus the identification of major minerals, minor minerals, and determination of rock texture, rough mineral proportions, and mineral chemistry [*Haskin et al.*, 1997]. Below, we discuss some properties of the current MMRS brassboard. Then, we describe its performance on several types of targets.

2.1. Raman Spectroscopy

[8] In Raman spectroscopy, monochromatic light (λ_0) from a source is scattered inelastically from the target material, for example, a mineral [*Long*, 1977]. The spectrometer rejects reflected light from the source and Rayleigh-scattered light of that same wavelength (λ_0), and it analyzes the longer wavelengths of the Raman-scattered light (Stokes lines, $\lambda_0 + \Delta\lambda$). The difference in wavelength between the source light and the scattered light corresponds to transition energies in the material that produced the scattering. This difference in wavelength, $\Delta\lambda$, normally given in units of wave number, cm^{-1}, is called the ''Raman shift.'' For example, inelastic scattering from the silicate mineral olivine gives Raman-scattered light of several principal wavelengths, and those wavelengths are characteristic of olivine. The transitions that give rise to these main peaks are Si-O vibrational motions, transitions whose energies correspond to those of midinfrared and far-infrared

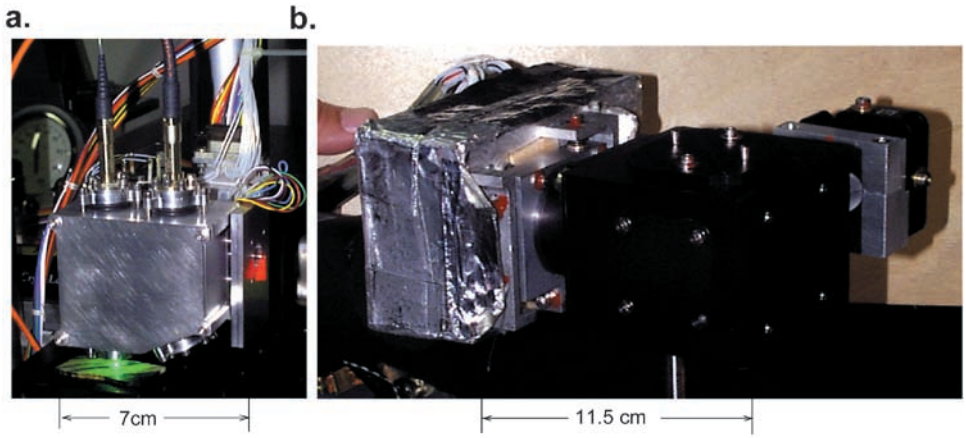

Figure 1. (a) The probe of the MMRS brassboard suspended above a small laboratory jack on which the sample rests. Although the laser beam is narrow (~28 μm) at the sample, multiple reflections give the pool of green light seen in the figure. (b) The MMRS spectrograph (black) is attached to a laboratory cooling box (covered with aluminum foil) to chill the CCD; on Mars, such a cooler will not be needed.

photons. For many minerals, a plethora of minor peaks is also produced. A technological advantage of Raman spectroscopy is that it provides information similar to that obtained by midinfrared and far-infrared spectroscopy, but the spectra can be obtained in the visible spectral region where Raman spectroscopy is efficient. Also, lasers and detection systems in the visible region of the spectrum are well understood and have space flight heritage because most optical and electro-optical components have their best performances there and have a long history of successful fabrication.

2.2. Selection of Excitation Wavelength and Lasers

[9] Because the Raman effect is weak, a laser excitation source is required for practical for use. Shorter excitation wavelengths are the most effective for a given laser power because of the $1/\lambda^4$ dependence of Raman scattering intensity. For an on-surface planetary application, small volume

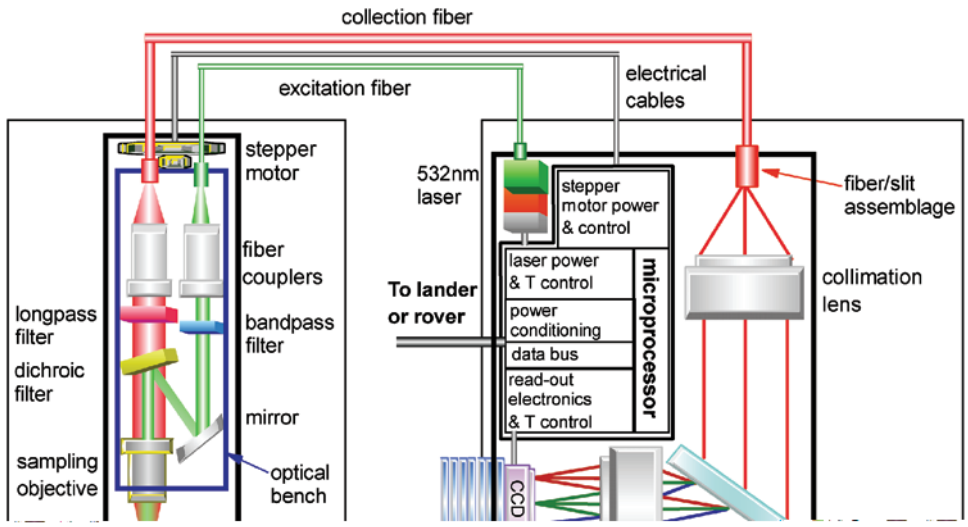

Figure 2. A schematic diagram of the probe, spectrograph, and ancillary units as they would be distributed between a mechanical arm and the rover or lander body in a spacecraft application. The diagram shows the optical components, their relative positions, and the light path. Power comes to the system from the host rover or lander and is conditioned by the instrument. Data for the set of spectra are sent from the microprocessor to the host for transmission to Earth. The probe shell is shown pressed against the uneven surface of a rock. The scanning motion of the optical bench within the probe shell is perpendicular to the page.

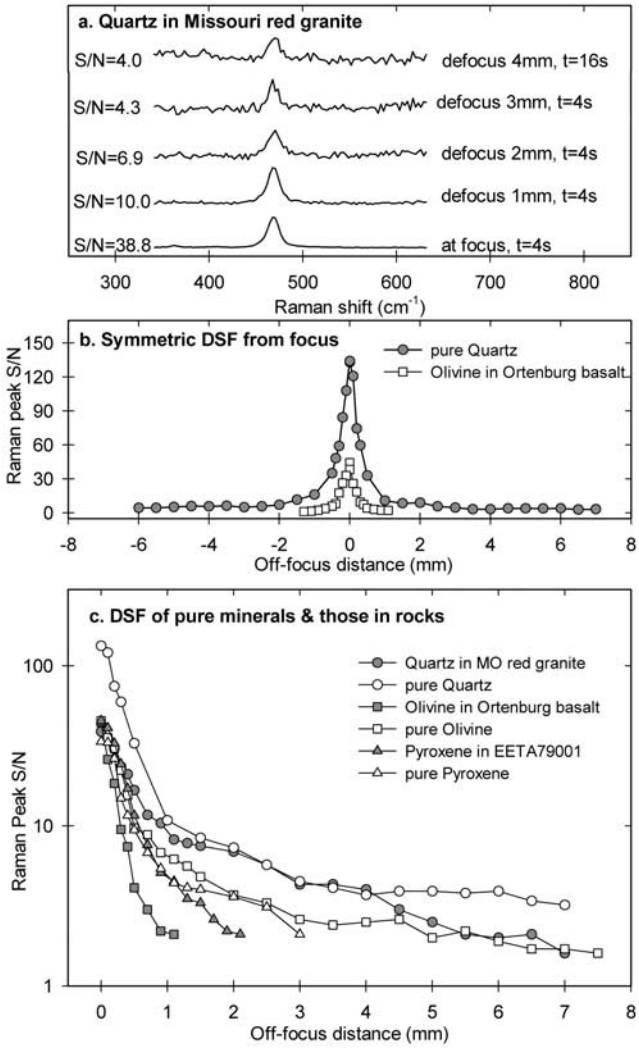

Figure 14. (a) The changes in the spectra that accompany defocusing of the instrument are shown for a favorable situation, quartz in the Missouri red granite. A substantial depth-of-sampling field (DSF) is crucial to compensate for target relief during measurements on rock or soil surfaces as encountered in the field. The spectra are shown in a manner to emphasize the decrease in S/N with increasing distance from the focal plane. (Note the expanded abscissa compared with that of previous figures.) (b) The signal-to-noise ratio for off-focus measurements is symmetric in both directions from focus, i.e., from below or from above the target focal point. This is shown for the single crystal of quartz and for a grain of olivine in the Ortenburg basalt. (c) Signal-to-noise ratios for mineral samples are less sensitive to off-focus distance than those for small mineral grains embedded in rock matrices, as seen here. The single-grain mineral samples are quartz, olivine, and pyroxene; the same as those in Figure 6. The mineral grains in rocks are quartz in the Missouri red granite, olivine in the Ortenburg basalt, and pyroxene in Martian meteorite EETA79001.

than those taken near the focus. This is more of a problem for intrinsically weak Raman scatterers than for strong ones, and the maximum off-focus distance for detecting weak scatterers is thus shorter than that for strong scatterers. An important factor that affects the distance for off-focus detection of a mineral is the nature of the matrix in which it resides and the grain size of that matrix. Off-focus measurements sample a larger area than on-focus measurements, and in a fine-grained material, off-focus measurements can involve Raman signal from several grains rather than just one or two. Thus, if the target is far enough out of focus, only strong scatterers may be detected even when a weak scatterer is within the illuminated volume. If at a particular location a strong scatterer is observed to have a weaker peak intensity than is common at other locations on the target, the location from which that spectrum was obtained may be significantly off focus. Also, if the matrix has a high level of fluorescent emission, or if the matrix is a strong absorber of the excitation laser wavelength, the Raman emission from a particular mineral grain in the matrix could be missed when a large area of matrix gets sampled in an off-focus measurement.

[48] We selected three major rock-forming minerals, quartz (colorless), olivine (moderately dark-colored), and pyroxene (dark-colored), to test the depth-of-sampling field of the MMRS brassboard. The test was made first on single, large mineral grains that contained the entire sampling volume of the Raman probe even at 7 mm off-focus. Then, a set of tests was made on the same minerals but on grains within rock samples: quartz of large grain size (several millimeters) in the Missouri red granite, olivine of smaller grain size (<1 mm) in the almost black Ortenburg basalt, and pyroxene of ~0.15 mm grain size in the gray Martian meteorite EETA79001. Sequential off-focus measurements were made by moving the Raman probe both toward and away from focus in increments of 100–500 μm. The spectra obtained when the probe was moved away from the Missouri red granite are shown in Figure 14a. The quartz spectrum is easily seen at all distances, but the integration times were necessarily longer for the spectra taken farthest from focus. The S/N of the Raman peaks, measured as peak height over the RMS value of the adjacent background, was used to evaluate the detection sensitivity of each mineral when measured off-focus. We observed no obvious difference in rate of change of the S/N in starting the sampling objective below the focal point as opposed to starting it above the focal point (Figure 14b). The S/N of the Raman spectra as a function of the off-focus distance is shown for all six sets of measurements in Figure 14c.

[49] The MMRS brassboard demonstrates an excellent depth-of-sampling field of at least ±7 mm for light colored, strong Raman scatterers such as quartz (carbonates and sulfates would be similar). We found no obvious difference between measurements on individual, isolated pure mineral grains and those on large grains in a light colored rock matrix, except at the farthest off-focus distances, where the large single mineral grains still contained the entire sampling volume but the mineral grain within the rock matrix did not. The depth-of-sampling field of ±2 mm is acceptable for medium strength Raman scatterers such as pyroxene (feldspar and other silicates would be similar) in a light colored rock matrix of fine grain size, as was observed for Martian meteorite EETA79001. Olivine has a fairly large grain size in the Ortenburg basalt and a slightly higher Raman scattering strength than pyroxene (compare the curves in Figure 14c for pure olivine and pure pyroxene).

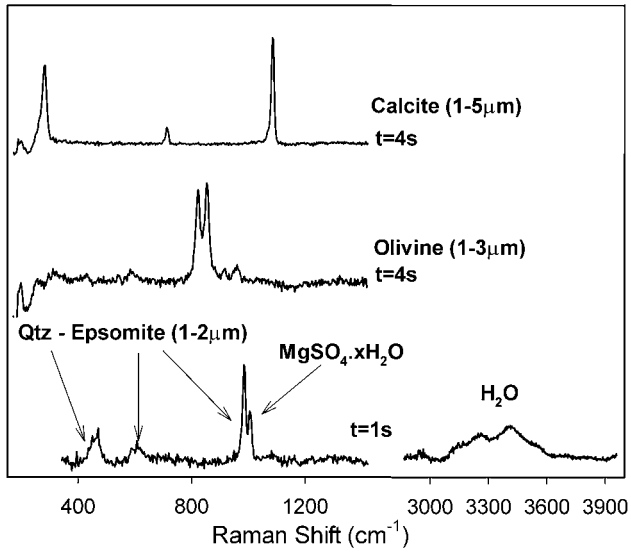

Figure 15. Raman spectra are shown of mineral specimens with a small grain size. The calcite and olivine grains were prepared by grinding larger grains and have grain-size distributions that peak at <1 μm in diameter but reach ~5 and ~3 μm. The epsomite was crystallized from an aqueous solution onto a matrix of fine-grained (~1 μm) quartz. Most of the epsomite grains have diameters in the 1–2 μm range. On standing in the laboratory, some of the epsomite began to lose water of hydration, giving rise to a second peak for both sulfate and water of hydration.

However, the depth-of-sampling field measured by the MMRS brassboard on olivine in Ortenburg basalt is actually shallower than that for pyroxene in EETA79001, only about ±1.2 mm. This appears to be an effect of the stronger competition from absorption in the much darker matrix of the Ortenburg basalt.

[50] Characterizing fine-grained materials on Mars is a challenge for all in situ or remote sensing instruments and that includes the MMRS. The magnitude of the grain size effect depends on the Raman scattering strength of each particular mineral. We have prepared different types of fine-grained samples. In one experiment, crystals of calcite and olivine were separately ground and sieved wet into the following size ranges: >250, 250–150, 150–75, 75–37.5, and <37.5 μm [*Wang*, 1999d]. We took spectra on the smallest of these using MMRS brassboard. In the <37.5 μm size fractions, most of the olivine grains are 1–3 μm in diameter and most of the calcite grains are in the 1–5 μm range [*Kuebler et al.*, 2001]. The measurements were made on heaps of these grains; thus, the effects of surface to volume ratio, porosity, multiple reflections at grain boundaries, and surface roughness are all present. The spectra from these samples are shown in Figure 15. The MMRS brassboard obtained good Raman signals from both samples. We do not observe a spectral pattern change or peak position shift in the Raman spectra of fine grains down to 1 μm, in contrast to some observations using Vis–Near-IR and Mid-IR spectroscopy [*Pieters*, 1983; *Pieters et al.*, 1993a, 1993b; *Lane*, 1999].

[51] Sulfur is abundant in the Martian soil, probably in the form of sulfates [*Clark and Van Hart*, 1981]. Sulfates may be present as evaporite minerals in the duricrust. We produced a simple form of pseudoduricrust by evaporating a solution of $MgSO_4$ onto a matrix of powdered, fine-grained quartz. The sulfate grain size was mostly ≤1 μm [*Kuebler et al.*, 2001]. In raw Raman spectra obtained using the MMRS brassboard (Figure 15), the major Raman peak (982 cm^{-1}) of freshly produced $MgSO_4 \cdot 7H_2O$ and minor peaks at lower Raman shift values were easily observed. The broad peak produced by OH vibrations in the bound H_2O molecules is also visible in the spectrum, but only after flat-field processing. On standing in the laboratory environment for several months, some of the $MgSO_4 \cdot 7H_2O$ was partially dehydrated. The additional peak at 950 cm^{-1} is from that less hydrated form.

4. MMRS Engineering Model

[52] The purpose of this paper has been to demonstrate that we can fabricate a miniaturized Raman spectrometer of near laboratory caliber suitable for use on a planetary surface mission, especially the surface of Mars. The results from the MMRS brassboard have enabled us to fulfill this purpose. One purpose of the MMRS brassboard was to demonstrate feasibility, but another is to progress toward the more sophisticated design that will lead to the actual flight instrument. The results of testing of the brassboard will be used in the design of the engineering model, which is the advanced prototype that will retire the technological risks associated with fabricating a flight instrument and which demonstrates the interfaces with the host rover or lander. These interfaces cannot be fully addressed until they have been specified at the host end, but general aspects of likely interfaces can be anticipated. Here, we list some issues and improvements that the engineering model development will incur. These improvements mainly involve more informed specifications of spectrometer components rather than further technological advances.

[53] A custom grating in the engineering model spectrograph will produce two spectral windows without overlap and will thus stretch the images on the CCD so that the spectral resolution is the desired 7 cm^{-1}. This will increase the wavelength precision of the spectra so that, combined with on-board wavelength calibration using an internal standard, Raman peak positions will be accurate and precise to 1–2 cm^{-1}, which will enable us to constrain more tightly the cation ratios of the minerals.

[54] The throughput of the spectrograph will be improved by a more precise alignment of the input fiber with the slit and by optimizing the lenses and coatings for transmission of wavelengths corresponding to Raman shifts from the green 532 nm wavelength. These changes are expected approximately to double the throughput of the spectrograph and thus the detection sensitivity.

[55] The filters that remove the reflected laser light and the Rayleigh-scattered light from the Raman signal will have a steeper slope between cutoff of the laser wavelength and transmittance of Raman-scattered photons. This will significantly increase the sensitivity of the instrument for Raman shifts in the 180–350 cm^{-1} range.

[56] From our experience with the MMRS brassboard, we are learning how to specify the software commands for autocontrol of integration time at each target point, in order to avoid saturation from photoluminescence, increase the

Raman S/N relative to photoluminescence, and to ensure adequate integration for weak Raman scatterers.

[57] Now that the efficacy of a small excitation laser of green wavelength has been proven, a specific laser and its configuration will be selected. This selection will improve the optical design of the probe. A narrower laser beam will be sent to the target, still retaining the effective depth-of-sampling field of several millimeters. The laser will also be operable in a low-power mode for detection of heat-sensitive minerals and in a higher-power mode for more robust minerals.

[58] In summary, the present brassboard of MMRS reaches ~20% of the detection sensitivity of our state-of-the-art laboratory Raman system with slightly poorer spectral resolution. The above improvements will at least double the sensitivity and improve the spectral resolution.

[59] **Acknowledgments.** This work was supported by NASA grants NAG5-7140 and NAG5-10703. We gratefully acknowledge contributions to the development of this instrument provided by the following individuals and their organizations: Jose Apodaca, Joel Johnson, Gordon Mon, Olga Shchedrin, and Jim Shea of the Pasadena Office of the Swales Aerospace Corporation for optical, mechanical, and thermal design; James Arns of Kaiser Optical Systems, Inc. for grating design; Boris Shnapir of Barr Associates for filter design; and Mark Wadsworth and Tom Elliot of the Jet Propulsion Laboratory for CCD detector selection and testing, with component assistance from the Phillips Corporation. Important individual contributions came from Matt Novak, Siamak Forouhar, Gindi French, Curtis Keedy, Joe Mansour, John Johnston, and Kai Zhu of the Jet Propulsion Laboratory.

References

Arns, J. A., Holographic transmission grating improve spectroscopy and ultrafast laser performance, *SPIE Proc.*, *2404*, 174–181, 1995.

Battey, D. E., J. B. Slater, R. Wludka, H. Owen, D. M. Pelletier, and M. D. Morris, Axial transmissive f/1.8 imaging Raman spectrograph with volume-phase holographic filter and grating, *Appl. Spectrosc.*, *47*, 1913–1919, 1993.

Bell, J. F., III, Iron, sulfate, carbonate, and hydrated minerals on Mars, in *Mineral Spectroscopy: A Tribute to Roger G. Burns, Geochem. Soc. Spec. Publ.*, vol. 5, edited by M. D. Dyar et al., pp. 359–380, Geochemical Soc., Houston, Texas, 1996.

Bell, J. F., et al., Minerologic and compositional properties of Martian soil and dust: Results from Mars Pathfinder, *J. Geophys. Res.*, *105*, 1721–1755, 2000.

Brannon, J. C., Geochemistry of successive lava flows of the Keweenawan North Shore Volcanic Group, Ph.D. dissertation, Washington Univ., St. Louis, MO, 1984.

Christensen, P. R., et al., Mars Global Surveyor Thermal Emission Spectrometer experiment: Investigation description and surface science results, *J. Geophys. Res.*, *106*, 23,823–23,871, 2001.

Clark, B. C., and D. C. Van Hart, The salt of Mars, *Icarus*, *45*, 370–378, 1981.

Cooney, T. F., H. T. Skinner, and S. M. Angel, Comparative study of some fiber-optic remote Raman probe designs, part 1, Models for liquids and transparent solids, *Appl. Spectrosc.*, *50*, 836–848, 1996.

Cooney, T. F., H. T. Skinner, and S. M. Angel, Comparative study of some fiber-optic remote Raman probe designs, part 2, Tests of single-fiber, lensed, and flat- and bevel-tip multi-fiber probes, *Appl. Spectrosc.*, *50*, 849–860, 1996.

Cooney, T. F., E. R. D. Scott, A. N. Krot, S. K. Sharma, and A. Yamaguchi, Vibrational spectroscopic study of minerals in the Martian meteorite ALH84001, *Am. Mineral.*, *84*, 1569–1576, 1999.

Dhamelincourt, P., and J. Barbillat, Raman microscopy, in *Handbook of Microscopy: Methods I*, Chap. 5, edited by S. Amelinckx et al., p. 54, John Wiley, New York, 1997.

Dickensheets, D., D. D. Wynn-Williams, H. G. M. Edwards, C. Schoen, C. Crowder, and E. M. Newton, A novel miniature confocal microscope/Raman spectrometer system for biomolecular analysis on future Mars missions after Antarctic trials, *J. Raman Spectrosc.*, *31*, 633–635, 2000.

Edwards, H. G. M., D. W. Farwell, M. M. Grady, D. D. Wynn-Williams, and I. P. Wright, Comparative Raman spectroscopy of a Martian meteorite and Antarctic lithic analogues, *Planet. Space Sci.*, *47*, 353–362, 1999.

Exobiology Program Office, NASA HQ, An exobiological strategy for Mars exploration, *NASA Spec. Pap. SP, 530*, 1995.

Fagan, T. J., E. R. D. Scott, K. Keil, T. F. Cooney, and S. K. Sharma, Formation of feldspathic, metallic, and enstatitic melts by shock in enstatite chondrite Reckling Peak A80259, *Meteorit. Planet. Sci.*, *35*, 319–329, 2000.

Fonti, S., A. Jurewicz, A. Blanco, M. I. Blecka, and V. Orofino, Presence and detection of carbonates on the Martian surface, *J. Geophys. Res.*, *106*, 27,815–27,822, 2001.

Guyot, F., H. Boyer, M. Madon, B. Velde, and J. P. Poirier, Comparison of the Raman microprobe spectra of $(Mg,Fe)_2SiO_4$ and Mg_2GeO_4 with olivine and spinel structures, *Phys. Chem. Miner.*, *13*, 91–95, 1986.

Hargraves, R. B., J. M. Knudsen, P. Bertelsen, W. Goetz, H. P. Gunnlauggsson, S. F. Hviid, M. B. Madsen, and M. Olsen, Magnetic enhancement on the surface of Mars?, *J. Geophys. Res.*, *105*, 1819–1827, 2000.

Haskin, L. A., A. Wang, K. M. Rockow, B. L. Jolliff, R. L. Korotev, and K. M. Viskupic, Raman spectroscopy for mineral identification and quantification for in-situ planetary surface analysis: A point count method, *J. Geophys. Res.*, *102*, 19,293–19,306, 1997.

Kargel, J. S., K. L. Tanaka, V. R. Baker, G. Komatsu, and D. R. MacAyeal, Formation and dissociation of clathrate hydrates on Mars: Polar caps, northern plains, and highlands, *Lunar Planet. Sci.*, *XXXI*, abstract 1891, 2000.

Klingelhöfer, G., The miniaturized spectrometer MIMOS II: The 2001 and 2003 US Mars missions and terrestrial applications in materials science and industry, in *Mossbauer Spectroscopy in Materials Sciences*, edited by M. Miglierini and D. Petridis, Kluwer Acad., Norwell, Mass., 1999.

Komatsu, G., J. S. Kargel, V. R. Baker, R. G. Strom, G. G. Ori, C. Modangini, and K. L. Tanaka, A chaotic terrain formation hypothesis: Explosive outgas and outflow by dissociation of clathrate on Mars, *Lunar Planet. Sci.*, *XXXI*, abstract 1434, 2000.

Kuebler, K. E., A. Wang, K. Abbott, and L. A. Haskin, Can we detect carbonate and sulfate minerals on the surface of Mars by Raman spectroscopy?, *Lunar Planet. Sci.*, *XXXII*, abstract 1889, 2001.

Kudryavtsev, A. B., J. W. Schopf, D. G. Agresti, and T. J. Wdowiak, In situ laser imagery of Precambrian microscopic fossils, *Proc. Natl. Acad. Sci.*, *98*, 823–826, 2001.

Lane, M. D., Midinfrared optical constants of calcite and their relationship to particle size effects in thermal emission spectra of granular calcite, *J. Geophys. Res.*, *104*, 14,099–14,108, 1999.

Long, D. A., *Raman Spectroscopy*, pp. 2–5, McGraw-Hill, New York, 1977.

Longhi, J., Low-temperature phase relations in the CO_2–H_2O system with application to Mars, *Lunar Planet. Sci.*, *XXXI*, abstract 1518, 2000.

Longhi, J., Clahtrate and ice stability in a porous Martian regolith, *Lunar Planet. Sci.*, *XXXII*, abstract 1955, 2001.

Madsen, M. B., S. F. Hviid, H. P. Gunnlauggsson, J. M. Knudsen, W. Goetz, C. T. Pedersen, A. R. Dinesen, C. T. Mogensen, and M. Olsen, The magnetic properties experiments on Mars Pathfinder, *J. Geophys. Res.*, *104*, 8761–8779, 1999.

McSween, H. Y., Jr., and E. Jarosewich, Petrogenesis of the Elephant Moraine A79001 meteorite: Multiple magma pulses on the shergottite parent body, *Geochim. Cosmochim. Acta*, *47*, 1501–1513, 1983.

Morris, R. V., et al., Mineralogy, composition, and alteration of Mars Pathfinder rocks and soils: Evidence from multispectral, elemental, and magnetic data on terrestrial analogue, SNC meteorite, and Pathfinder samples, *J. Geophys. Res.*, *105*, 1757–1817, 2000.

Morris, R. V., D. C. Golden, D. W. Ming, T. D. Shelfer, L. C. Jorgensen, J. F. Bell III, T. G. Graff, and S. A. Mertzman, Phyllosilicate-poor palagonitic dust from Mauna Kea Volcano (Hawaii): A mineralogical analogue for magnetic Martian dust, *J. Geophys. Res.*, *106*, 5057–5083, 2001.

Pieters, C. M., Strength of mineralogical absorption features in the transmitted component of reflection: First results from RELAB, *J. Geophys. Res.*, *88*, 9534–9544, 1983.

Pieters, C. M., E. M. Fischer, O. Rode, and A. Basu, Optical effects of space weathering: The role of the finest fraction, *J. Geophys. Res.*, *98*, 20,817–20,824, 1993a.

Pieters, C. M., J. F. Mustard, S. F. Pratt, J. M. Sunshine, and A. Hoppin, Visible infrared properties of controlled laboratory soils, *Proc. Lunar Planet. Sci. Conf.*, *XXIV*, 1147–1148, 1993b.

Rieder, R., H. Wänke, T. Economou, and A. Turkevich, Determination of the chemical composition of Martian soils and rocks: The alpha proton X-ray spectrometer, *J. Geophys. Res.*, *102*, 4027–4044, 1997.

Schoen, C. L., T. F. Cooney, S. K. Sharma, and D. M. Carey, Long fiber-optic remote Raman probe for detection and identification of weak scatterers, *Appl. Opt.*, *31*, 7707–7715, 1992.

Sharma, S. K., C. L. Schoen, and T. F. Cooney, Fiber-optic remote Raman probe design for use in monitoring processes in a high-temperature oven, *Appl. Spectrosc.*, *47*, 377–379, 1993.

Squyres, S. W., et al., The Mars 2001 Athena Precursor Experiment (APEX), *Lunar Planet. Sci.*, *XXX*, abstract 1672, 1999.

Soderblom, L. A., The composition and mineralogy of the Martian surface from spectroscopic observations: 0.3 μm to 50 μm, in *Mars*, Chapter 17, edited by H. H. Kieffer et al., pp. 557–593, 1498 pp., Univ. of Ariz. Press, Tucson, 1992.

Sum, A. K., R. C. Burruss, and E. D. Sloan, Jr., Measurement of clathrates via Raman spectroscopy, *J. Phys. Chem.*, *B101*, 7371–7377, 1997.

Walsh, M. M., and D. R. Lowe, Modes of accumulation of carbonaceous matter in the early Archean: A petrographic and geochemical study of the carbonaceous cherts of the Swaziland Supergroup, in *Geologic Evolution of the Barberton Greenstone Belt, South Africa, Spec. Pap. Geol. Soc. Am.*, vol. 32, edited by D. R. Lowe and G. R. Byerly, pp. 115–132, Geol. Soc. of Am., Boulder, 1999.

Wang, A., Some grain size effects on Raman scattering intensity for in situ measurements on rocks and soils: Experimental tests and modeling, *Lunar Planet. Sci.*, *XXX*, abstract 1644, 1999.

Wang, A., and R. B. Valentine, Seeking and identifying phyllosilicates on Mars: A simulation study, *Lunar Planet. Sci.* [CD-ROM], *XXXIII*, abstract 1370, 2002.

Wang, A., J. Han, L. Guo, J. Yu, and P. Zeng, A database of standard Raman spectra of mineral and related inorganic crystals, *Appl. Spectrosc.*, *48*, 959–968, 1994.

Wang, A., B. L. Jolliff, and L. A. Haskin, Raman spectroscopy as a method for mineral identification on lunar robotic exploration missions, *J. Geophys. Res.*, *100*, 21,189–21,199, 1995.

Wang, A., L. A. Haskin, and E. Cortez, A Raman spectroscopic sensor for in situ mineral characterization on planetary surface, *Appl. Spectrosc.*, *52*, 477–487, 1998a.

Wang, A., L. A. Haskin, and B. L. Jolliff, Characterization of mineral products of oxidation and hydration by laser Raman spectroscopy: Implications for in situ petrologic investigation on the surface of Mars, *Lunar Planet. Sci.*, *XXVIII*, abstract 1819, 1998b.

Wang, A., B. L. Jolliff, and L. A. Haskin, Raman spectroscopic characterization of a highly weathered basalt: Igneous mineralogy, alteration products, and a micro-organism, *J. Geophys. Res.*, *104*, 27,067–27,077, 1999a.

Wang, A., B. L. Jolliff, and L. A. Haskin, Raman spectroscopic characterization of a Martian SNC meteorite Zagami, *J. Geophys. Res.*, *104*, 8509–8519, 1999b.

Wang, A., B. L. Jolliff, L. A. Haskin, and K. E. Kuebler, Raman spectral features of pyroxene: Application to Martian meteorites Zagami & EETA79001, *Lunar Planet. Sci.*, *XXX*, abstract 1666, 1999c.

Wang, A., K. E. Kuebler, B. L. Jolliff, and L. A. Haskin, Mineral features of EETA79001 Martian meteorite revealed by point-counting Raman measurements as anticipated for in-situ exploration on planetary surfaces, *Lunar Planet. Sci.*, *XXXI*, abstract 1887, 2000.

Wang, A., K. E. Kuebler, and B. L. Jolliff, Raman spectroscopy of opaque minerals and applications to EETA79001 Martian meteorite, *Lunar Planet. Sci.*, *XXXII*, abstract 1615, 2001a.

Wang, A., L. A. Haskin, K. E. Kuebler, B. L. Jolliff, and M. M. Walsh, Raman spectroscopic detection of graphitic carbon of biogenic parentage in an ancient South African chert, *Lunar Planet. Sci.*, *XXXII*, abstract 1432, 2001b.

Wang, A., B. L. Jolliff, L. A. Haskin, K. E. Kuebler, and K. M. Viskupic, Characterization and comparison of structural and compositional features of planetary quadrilateral pyroxenes by Raman spectroscopy, *Am. Mineral.*, *86*, 790–806, 2001c.

Wang, A., J. Freeman, and K. E. Kuebler, Raman spectroscopic characterization of phyllosilicates, *Lunar Planet. Sci.*, *XXXIII*, abstract 1374, 2002.

Wopenka, B., and J. D. Pasteris, Structural characterization of kerogens to granulite-facies graphite: Applicability of Raman microprobe spectroscopy, *Am. Mineral.*, *78*, 533–557, 1993.

Wynn-Williams, D. D., and H. G. M. Edwards, Proximal analysis of regolith habitats and protective biomolecules in situ by laser Raman spectroscopy: Overview of terrestrial Antarctic habitats and Mars analogs, *Icarus*, *144*, 486–503, 2000.

Yen, A. S., S. S. Kim, M. H. Hecht, M. S. Frant, and B. Murray, Evidence that reactivity of the Martian soil is due to superoxide ions, *Nature*, *289*, 1909–1912, 2000.

L. A. Haskin and A. Wang, Department of Earth and Planetary Sciences and McDonnell Center for the Space Sciences, Washington University, One Brookings Drive, St. Louis, MO 63130, USA. (alianw@levee.wustl.edu)

L. E. Hovland, A. L. Lane, K. S. Manatt, N. Raouf, and R. J. Wilson, Jet Propulsion Laboratory, 4800 Oak Grove Drive, Pasadena, CA 91109, USA.

C. D. Smith, Swales Aerospace Corp., 404 N. Halstead Street, Pasadena, CA 91107, USA.

S. W. Squyres, Center for Radiophysics and Space Physics, Cornell University, Ithaca, NY 14853, USA.

T. J. Wdowiak, Department of Physics, University of Alabama at Birmingham, Birmingham, AL 35294-1170, USA.